Available online at www.sciencedirect.com
ScienceDirect
Journal of Nuclear Materials 367–370 (2007) 1404–1409
journal of nuclear materials
www.elsevier.com/locate/jnucmat

Verification of design rules for EUROFER under TBM operating conditions

R. Sunyk *, J. Aktaa

Forschungszentrum Karlsruhe, Institut für Materialforschung II, Hermann-von-Helmholtz-Platz 1, D-76344 Eggenstein-Leopoldshafen, Germany

Abstract

The aim of the activity presented in this work is, firstly, an evaluation of existing design rules considered for austenitic steels exhibiting cycle-by-cycle hardening, in contrast to the reduced-activation ferritic–martensitic steels (RAFM), which soften under cyclic loading. Secondly, we are aimed in a definition of the range of operating temperatures and loads for the current design of the test blanket module (TBM). Results of cycling tests of the EUROFER 97 have been thereby used to adjust material parameters needed for an ABAQUS-own combined non-linear isotropic–kinematic hardening model. Furthermore, a visco-plastic material model considering material damage and implemented recently as an ABAQUS user material (UMAT) has been also applied for simulations. Some important design rules within the elastic route have been evaluated and their predictions have been compared to results of cyclic simulations using the advanced material models mentioned above.

1. Introduction

This work is a part of the development activity of the ITER test blanket module (TBM). A determination of high-temperature design rules considering creep/fatigue is the aim of this activity. According to the present-day vision, the TBM should be manufactured from a reduced-activation ferritic–martensitic (RAFM) steel EUROFER 97, which exhibits severe softening during cyclic loading, in contrast to the austenitic steels. This abnormal behavior leads to a necessity to revise the traditional formulation of some important design rules, especially related to the protection against the c-type damage such as the well-known $3S_m$ rule.

Such a revision requests, firstly, a wide experimental data base and, secondly, an advanced material model able to describe the realistic behavior of the material. The fulfillment of both these requirements as well as acute needs of blanket designers for renewed rules thus form positive initial conditions for the appearance of the results, presented in this publication.

We have recently reported the results of first simulations using the advanced materials models, see [1].

2. Adjustment of material parameters

To simulate the actual behavior of the TBM under cyclic thermal and mechanical loading,

* Corresponding author. Tel.: +49 7247 82 4569; fax: +49 7247 82 4566.
E-mail address: Rudolf.sunyk@imf.fzk.de (R. Sunyk).

0022-3115/$ - see front matter © 2007 Published by Elsevier B.V.
doi:10.1016/j.jnucmat.2007.04.041

experimental data of corresponding cyclic tests are needed. Such data stemming from a life time study of the EUROFER 97 at 450 °C (723 K), 550 °C (823 K) and 650 °C (923 K) performed by Aktaa and Schmitt [2] as well as at the room temperature (RT) provided by Weick [3] have been used to adjust material parameters required for an ABAQUS-own non-linear isotropic–kinematic hardening model [4]. This model is able to account e.g., for the Bauschinger effect, cyclic hardening/softening with plastic shakedown as well as for ratcheting. A description of the material model is given in [4] and is not repeated in this paper.

3. Determination of the elastic limit

3.1. Finite element model

To verify the material model described above, a 2D model of a quarter of the TBM has been created according to the current design and meshed using PATRAN. The model is shown in Fig. 1 together with mechanical constraints. The only external mechanical load in the non-accident operating mode is the hydrostatic pressure of 80 bar = 8 MPa in all cooling channels.

For those simulations where thermal stresses occur, ABAQUS provides a so called generalized plane strain element formulation, which accounts for an elongation in the out-of-plane direction and thus avoids enormously high non-physical out-of-plane stresses. The 8-node generalized plane strain elements CPEG8 have been used here.

3.2. Thermal simulation

During the operating mode, the model must account for a heat flux of 250 up to 500 kW/m^2 (peak) on the plasma-facing side as well as a heat flux of 60 kW/m^2 and of 35 kW/m^2 on the vertical and horizontal interior, respectively, due to breeder units, see Fig. 1. For reason of simplicity, temperature boundary conditions depicted in Fig. 1 have been considered in the simulations.

In order to determine acceptable loads, the behavior of the TBM should be simulated under consideration of different temperature distributions. To obtain such distributions, thermal simulation has been performed for four values of plasma heating: 250 kW/m^2 (the usual operating mode), 500 kW/m^2, 750 kW/m^2 and 1000 kW/m^2, as well as for three different temperatures in the cooling channels (T^{cc}): 673 K, 773 K and 873 K. The heating due to the breeder unit remains thereby constant. As an example of the typical temperature distribution, results of a thermal computation for the peak plasma heating and $T^{cc} = 773$ K are shown also in Fig. 1.

3.3. Mechanical simulations using various plasma heating and pressure in cooling channels (no cycling)

By variation of both the temperature in cooling channels and the plasma heating, a critical pressure has been determined based on both material models. The critical pressure is thereby defined as the minimum pressure causing any inelastic defor-

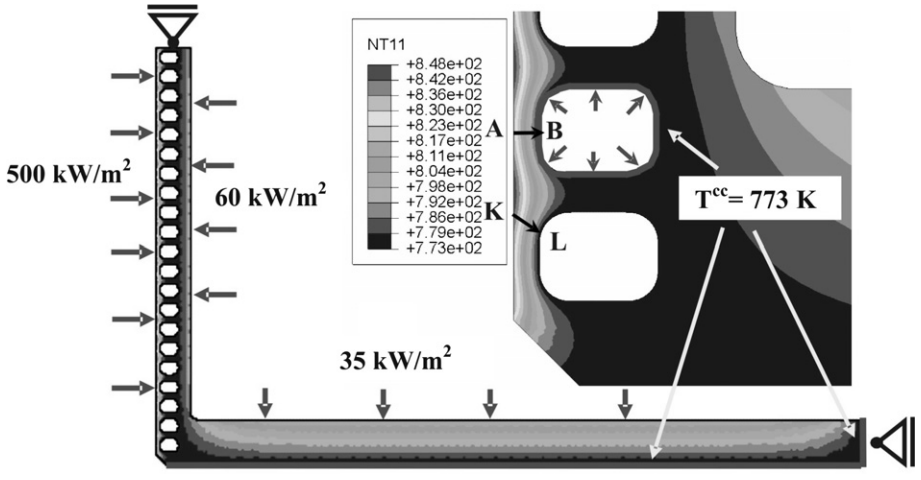

Fig. 1. The FE model of the TBM with mechanical and thermal constraints and loadings; temperature distribution (in K) due to the depicted thermal constraints and loads.

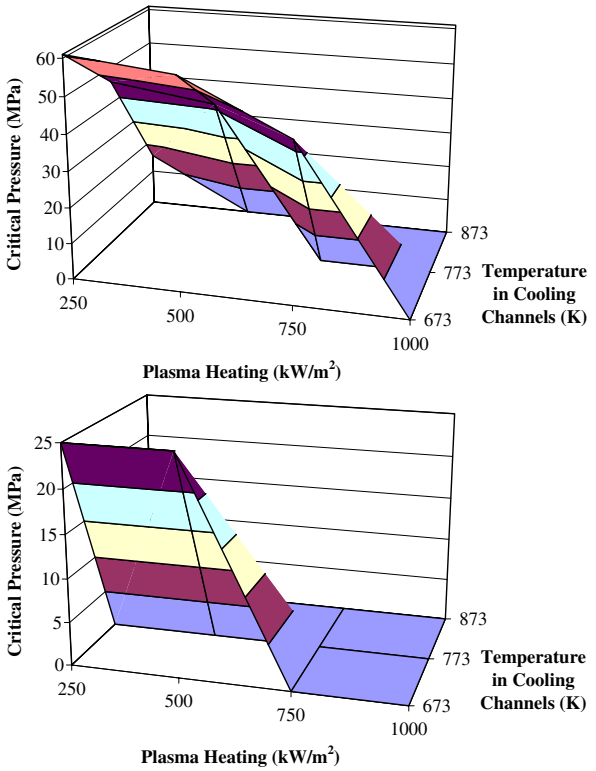

Fig. 2. The critical pressure as a function of the plasma heating and the temperature in cooling channels obtained using the ABAQUS-own material model (upper figure) and the UMAT (lower figure).

mation after the first heating i.e., after half of the first cycle for the ABAQUS-own material model and after the whole first cycle for the visco-plastic material model considering damage and implemented recently by Aktaa as a UMAT, see [2].

The critical pressure is shown in Fig. 2 for both material models as a function of the plasma heating and the temperature in the cooling channels T^{cc}. An application of the UMAT leads to more conservative results, which are probably more correct due to taking into account the high-temperature creep.

4. Simulations of the cyclic behavior of TBM

The cyclic behavior of the TBM model has been studied again using both the ABAQUS-own material model described above and the UMAT. Thereby, the following load case has been used: $T^{cc} = 600$ °C (873 K); the plasma heating 750 kW/m^2 and the coolant pressure $P = 50$ MPa (500 bar). It was assumed on the basis of the study reported in the previous section that such abnormal high loads should cause an important amount of inelastic deformation.

Each cycle consists of four steps: (1) heating and application of the pressure, 30 s; (2) holding at the high temperature (HT), 400 s, (3) cooling to RT, 100 s and, finally (4) holding at RT for 1400 s. Note that the steps (2) and (4) are not relevant for the ABAQUS-own time-independent material model.

We have simulated a few hundred cycles using both material models (300 with the ABAQUS-own material and 600 with the UMAT). Because of the high computing time and huge memory capacity needed, it seems unrealizable to continue such a simulation until the material fails (approximately 6000–10 000 cycles). Fortunately, the method proposed in [5] allows the simulation of such number of cycles by extrapolation of simulation data. However, it is a challenge for a further activity. The results have been generated in a table format along the paths AB and KL depicted in Fig. 1. A follow-up examination has shown that the highest plastic strain in the model occurs near the point L of the path KL. A change of the maximum equivalent plastic strain near the point L within the first 300 and 600 cycles is depicted in Fig. 3 for the ABAQUS-own material and the UMAT, respectively. A detailed investigation shows an almost linear increase of the equivalent plastic strain in the case of the ABAQUS-own material model. However, the increase lies between 1.355×10^{-3} and 1.366×10^{-3} for the first 300 cycle.

The application of the UMAT leads to considerably higher plastic strains due to the creep and damage of the material. Note that the values of the variable PEMAG (the magnitude of the plastic

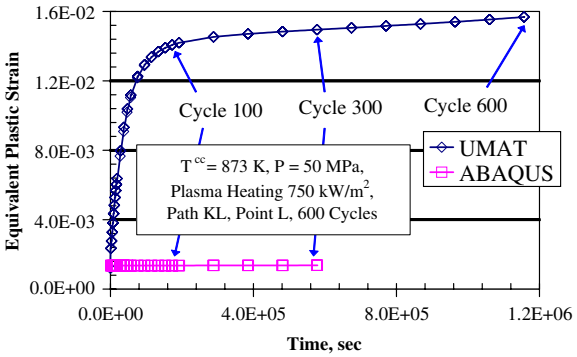

Fig. 3. The change of the maximum equivalent plastic strain among all values along the path KL, see Fig. 1, cycle by cycle during the first 300 cycles computed using the ABAQUS-own material and 600 cycles using the UMAT.

strain) after the first heating are quite similar for both models, see Fig. 3.

As follows from the curve depicted in Fig. 3, the magnitude of the plastic strain seems to reach a saturated value. However, to get a definite answer, the extrapolation method proposed in [5] should be applied. Only the more conservative results obtained based on the application of the UMAT are used below for the verification of some design rules.

5. Verification of design rules

The aim is now to compare the results discussed above with a prediction of some design rules based on linear-elastic simulations. To apply the design rules, some combinations of stress components should be compared with allowable stress intensities like S_m, which is the lowest stress intensity at a given temperature among the time-independent strength quantities, see ITER SDC-IC [6, Subsection IC 2723].

5.1. Calculation of S_m^*

The available S_m values do not consider a change of the tensile strength and yield stress cycle by cycle. This change can however be taken into account if S_m is calculated on the basis of the experimental data reported by Aktaa and Schmitt in [2]. Thereby, the maximum achieved tensile stress must be used here for calculations instead of the ultimate tensile strength. To obtain the needed tensile strengths and to enhance therewith the values of S_m^* reported below, monotonic tensile tests should be performed after e.g., 10, 20 etc. cycles.

The new value, calculated in such manner, is represented in Fig. 4 (labeled as EXP) together with the S_m values from ITER SDC-IC [6, Appendix A]. It was assumed that each cycle is 1930 s = 0.54 h long. To avoid a misunderstanding, the value has been labeled as S_m^*. Note that any stress leads to plastic collapse after 200 cycles at 650 °C (923 K). As follows from the diagrams in Fig. 4, ITER SDC-IC [6, Appendix A] provides too high values of S_m if the material experiences cyclic loading.

5.2. Stress categorization

To separate primary and secondary stresses, linear-elastic simulations have been performed for three load cases: thermal and mechanical loads acting together and separated. A comparison of the results obtained allows the recognition that the influence of plasma heating is partially compensated by the coolant pressure.

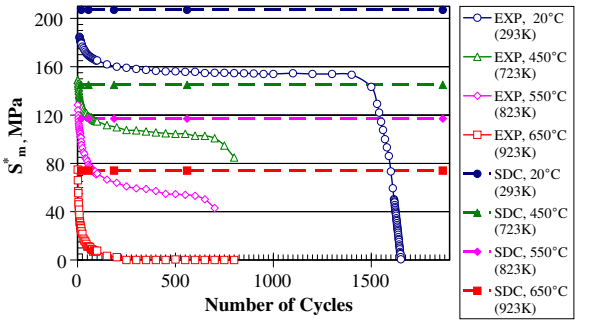

Fig. 4. Change of S_m^* under cyclic loading at RT, 450 °C (723 K), 550 °C (823 K) and 650 °C (923 K); available data for these temperatures stemming from ITER SDC-IC [6, Appendix A] are also given for comparison.

Results of these simulations have been linearized automatically along the paths discussed above using the corresponding option of the ABAQUS VIEWER.

5.3. Application of design rules

Within the frame of the work presented, the following low-temperature design rules have been checked:

- Rules for prevention of immediate plastic collapse and plastic instability (M-type damage)

$$\overline{P_m} \leqslant S_m,\ \overline{P_m + P_b} \leqslant KS_m, \tag{1}$$

- The rule for prevention of progressive deformation or ratcheting (C-type damage)

$$\overline{P_m + P_b} + \left[\overline{\Delta P}_{max} + \overline{\Delta Q}_{max}\right] \leqslant 3S_m, \tag{2}$$

where K is the bending shape factor, which ranges in general between 1.0 and 2.0. A value of $K = 1.5$ was chosen. The more conservative rule accounting for possible embrittlement caused by irradiation is not considered here since the material tested is unirradiated. Besides this factor, the following conventional notations are used here: $\overline{P_m}$ and $\overline{P_m + P_b}$ denote the primary membrane stress intensity and the primary membrane and bending stress intensity excluding plasma disruption loadings, respectively; $\overline{\Delta Q}_{max}$ and $\overline{\Delta P}_{max}$ are the maximum in the thickness secondary (thermal) stress intensity range and the stress

Table 1
Maximum absolute values of the categorized stress components and their combinations among all values for the chosen paths together with the corresponding values of S_m; all data are given in MPa

$\overline{P_m}$	$S_m^{898\ K}$	$S_m^{*898\ K}$	$S_m^{873\ K}$	$S_m^{*873\ K}$
117.0	87.0	23.7	98.0	39.7
$\overline{P_m + P_b}$	$K * S_m^{898\ K}$	$K * S_m^{*898\ K}$	$K * S_m^{873\ K}$	$K * S_m^{*873\ K}$
179.7	130.5	35.5	147.0	59.5
$\overline{P_m + P_b} + \overline{\Delta Q}_{max}$	$3 * S_m^{898\ K}$	$3 * S_m^{*898\ K}$	$3 * S_m^{873\ K}$	$3 * S_m^{*873\ K}$
395.5	261.0	71.0	294.0	119

intensity range due to disruption loadings (here not considered). Furthermore, the low-temperature Bree-diagram rule has also been evaluated:

$$Y \leqslant \frac{1}{X} \quad \text{if } 0 \leqslant X \leqslant 0.5 \quad \text{or}$$
$$Y \leqslant 4[1 - X] \quad \text{if } 0.5 \leqslant X \leqslant 1.0. \tag{3}$$

Here, $X = \overline{P_m}/S_y$, $Y = \left[\overline{\Delta P}_{max} + \overline{\Delta Q}_{max}\right]/S_y$; S_y is the average of the minimum yield strength evaluated at the minimum and maximum thickness-averaged temperatures and fluences during the cycle calculated along the supporting line segments.

The maximum values required for evaluation of (1) and (2) are collected in Table 1. An easy comparison shows that none of the three criteria is fulfilled even for the S_m value stemming from ITER SDC-IC [6, Appendix A] at $T^{cc} = 600$ °C (873 K). If the S_m value at the average temperature along the path (approx. 625 °C or 899 K) is considered, the difference becomes more essential. The gap becomes however huge if S_m^* value for this temperature is used.

An application of (3) shows that the less conservative Bree-diagram rule is fulfilled for three different temperatures from 873 K to 923 K. Nevertheless, criterion (2) should also be satisfied to apply the high-temperature $3S_m$ rule, see ITER SDC-IC [6, Subsection IC3541.3].

Thus, the chosen design rules predict (a) the plastic collapse and plastic instability as well as (b) the probable accumulation of plastic deformation. The simulation results obtained using the visco-plastic material model that includes damage seem to show a shakedown. However, as mentioned above, to obtain a more definite result, the extrapolation method [5] should be applied and, on the other hand, all design criteria should be checked according to the scheme given in ITER SDC-IC [6, Subsection IC3030].

6. Conclusion and outlooks

In the present work, material parameters required for the non-linear kinematic–isotropic hardening ABAQUS-own material model have been determined. These parameters have been used together with a visco-plastic material model considering material damage to determine the coolant pressure causing plastic deformation as a function of the temperature in the cooling channels and plasma heating. Furthermore, the cyclic behavior of the TBM has been simulated using both material models.

On the other hand, some important low-temperature design rules have been applied to the model and their predictions have been compared with results of the cyclic simulations. It thereby turned out that the criterions are not fulfilled, even if the conventional value of S_m is used. The newly calculated value S_m^*, which is introduced similar to S_m but accounts for the cyclic softening of the EUROFER 97 steel leads to a larger gap between the target and actual results.

The results of the cyclic simulations exhibit neither plastic collapse nor ratcheting after the first 600 cycles. This discrepancy could mean that the criterions are possibly too conservative for EUROFER 97 and new design rules should be considered. The suggestion, however, requires a further in-depth study including a verification of all (elastic and elastic–plastic) design rules preventing both the M-type and C-type damage, consideration of the effects of irradiation, hydrogen effect, and corrosion effect by the coolant as well as the possible change in the actual TBM geometry.

Acknowledgements

We are grateful for the experimental data at the room temperature kindly given by Dr Ing. M. Weick. We would also thank Mrs G. Rizzy for her help in performing the FE simulations. The presented work has been partly supported by the European Fusion Development Agreement (EFDA).

References

[1] R. Sunyk, J. Aktaa, Evaluation of material design limits for TBM applications, 2005, in: IEEE/SOFE05 Proceedings, <http://216.228.1.34/Conf/sofe05/versions/64291/PID131414.pdf>.
[2] J. Aktaa, R. Schmitt, Fusion Eng. Des., corrected proof.
[3] M. Weick, private communication, Forschungszentrum Karlsruhe GmbH, 2004.
[4] ABAQUS/Standard User's Manual, v. 6.2, Hibbitt, Karlsson & Sorensen Inc., 2001, Vol. II (Chapter 11.2.2).
[5] H. Kiewel, J. Aktaa, D. Munz, Comput. Meth. Appl. Mech. Eng. 182 (2000) 55.
[6] ITER Structural Design Criteria for In-vessel Components (SDC-IC), ITER Doc. G 74 MA 8 01-05-28 W0.2 (internal project document distributed to the ITER Participants).